Article

Molecular Packing of Phenoxazine: A Combined Single-Crystal/ Crystal Structure Prediction Study

Martin Kaltenegger, Louis Delaive, Sai Manoj Gali, Patrick Brocorens, Oliver Werzer, Hans Riegler, Yves Henri Geerts, Roberto Lazzaroni, Roland Resel,* and Jie Liu

Cite This: *Cryst. Growth Des.* 2022, 22, 1548−1553

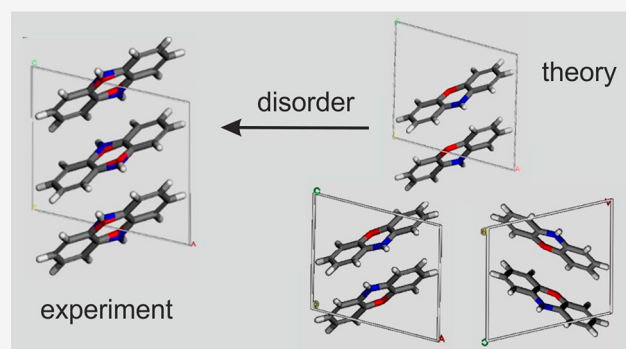Read Online

ACCESS | Metrics & More | Article Recommendations | Supporting Information

ABSTRACT: Phenoxazine is a heterocyclic molecule, which is used either as a parent molecule or with substituents for applications in various scientific fields: e.g., as a potential antioxidant. The purpose of this work is to present the molecular packing of phenoxazine within the crystalline state, as surprisingly no crystal structure is known so far. The crystal structure solution was performed by single-crystal X-ray investigations. Although the molecule has some potential for intermolecular hydrogen bonding, the observed structure is the classical herringbone packing typical for rodlike conjugated molecules. However, severe substitutional disorder of oxygen and nitrogen atoms is observed over their two opposite positions within the molecule. To get deeper insight into this disorder phenomenon, theoretical studies were performed, including crystal structure prediction using state of the art density functional theory techniques. The theoretical investigations confirm the experimentally observed 50% occupancy of the oxygen and nitrogen atoms.

■ INTRODUCTION

The compound of interest in this study is the small organic molecule phenoxazine (Figure 1), which is used in
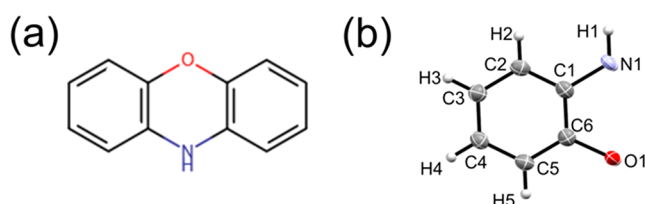

Figure 1. (a) Molecular structure of phenoxazine. The hydrogen atoms on the phenyls are omitted. (b) Asymmetric unit of phenoxazine as obtained from single-crystal diffraction. Displacement ellipsoids are drawn at the 50% probability level.

pharmaceutical research.[1,2] Often, phenoxazine works as a parent molecule and is found in different biological organisms.[1] Due to their widespread applications such as antioxidants, as antiviral, antibiotic, anticancer species, and many more, phenoxazine and its derivatives are important compounds in medicine.

Phenoxazine is a heterocyclic molecule that appears as a rigid and planar molecule. It consists of two phenyl rings connected by two covalent bridges. The connection is formed on one side by a bivalent oxygen atom and on the other side by a bivalent NH group. The presence of these two chemical

species at the center of the molecule makes the molecule prone to generating intermolecular hydrogen bonds. However, hydrogen bonds are quite difficult to prove for phenoxazine in the solid state, since the molecule has a symmetrical shape and the oxygen and nitrogen atoms are difficult to distinguish by X-ray diffraction techniques.

Interestingly, no crystal structure of phenoxazine has been reported in the literature so far, despite the fact that Geiger et al. reported the crystal structure of its complexes with *cis*-bis(trifluoronethylmethylene-1,2-dithioIato)nickel $(Ni(tfd)_2)$[3] and depicted that the disorder of the sites N and O suits a centrosymmetric space group. Several other organic crystals also display substitutional disorder.[4−6] In this work, we present the single-crystal structure of phenoxazine, which was determined by experimental diffraction data. It reveals a distinct disorder in the crystal structure in which one site is occupied by O and N atoms with a 50:50 probability.[7] Computational work for modeling disorder is able to support the experimentally determined crystal structures and lead to a better understanding of the molecular packing in the solid

form.[8−10] In this study, crystal structure prediction (CSP) was applied to generate possible efficient crystal structures and a density functional theory (DFT) method was used to refine the structure and energy.[11] The resultant computational structure is consistent with the experimental structure determined by X-ray diffraction. Given these results, a reliable understanding of the molecular packing in this disordered system was achieved.

■ EXPERIMENTAL SECTION

Sample Preparation. Phenoxazine was purchased from Sigma-Aldrich, Inc., with a purity of 97%. To grow a single crystal of phenoxazine, a 30 mg/mL THF solution was heated and filtered using a 0.22 μm PTFE filter. This solution was then placed in a 1 mL glass vessel enclosed with a Teflon seal that was pierced by a syringe needle, enabling slow solvent evaporation. The evaporation took more than 48 h. Single crystals grew upon evaporation and were harvested after all the solvent was gone.

X-ray Powder Diffraction. A powder sample was prepared from the as-delivered material and placed on a nonreflecting silicon wafer. An Empyrean diffractometer system (PANalytical, Netherland) equipped with a copper sealed tube (wavelength of 0.154 nm), a parallel beam mirror combined with a beam mask, and a divergence slit was used in combination with a PIXcel3D detector operating in integrating line mode.

Single-Crystal X-ray Diffraction. The synchrotron radiation facility Elettra, Trieste, Italy, offered access for our studies. At the beamline XRD1 single-crystal X-ray diffraction measurements were performed using a standard κ-geometry goniometer head with a wavelength of 0.700 Å. Diffraction data were collected at 100 K using a Pilatus 2 M (Dectris, Switzerland) detector. Data reduction was provided by the Elettra framework, including indexation and integration using XDS.[12] Scaling was done using the CCP4-Aimless code.[13,14] The crystal structure was solved by a direct method and refined by the full-matrix least-squares method on F^2 (SHELX-97).[15] All non-H atoms in the structure were refined with anisotropic thermal parameters, and the refinements converged for $I > 2\sigma(I)$.

Hirshfeld Surface Calculations. The Hirshfeld surface was calculated using the software CrystalExplorer 17.5.[16] The contact distance (d_{norm}) based on d_e (the distance from the point on the Hirshfeld surface to the nearest nucleus external to the surface) and d_i (the distance from the point on the surface to the nearest nucleus internal to the surface), normalized by van der Waals radii for the particular atoms involved in the close contact to the surface, is expressed as

$$d_{norm} = \frac{d_i - r_i^{vdw}}{r_i^{vdw}} + \frac{d_e - r_e^{vdw}}{r_e^{vdw}} \tag{1}$$

where r_i^{vdw} and r_e^{vdw} are the van der Waals (vdW) radii of the atoms. d_{norm} is represented by a surface with a red (distances shorter than sum of vdW radii) through white to blue (distances longer than the sum of vdW radii) colored graph. A 2D fingerprint plot defined by the frequency of each combination of d_e and d_i over the Hirshfeld surface reveals visually the contribution from different intermolecular contacts with a color from blue to green to red to reflect an increase in frequency.

Theoretical Investigations. Crystal structure prediction (CSP) was carried out using a combination of a force-field (FF) method to generate thousands of candidate structures and a density functional theory (DFT) method to refine the structure and energy of the best candidates generated with the force field. Such a hybrid CSP technique allows a reduction in the number of candidates to those present in an energy window of 4.2 kJ/mol.[17,18] To create thousands of random molecular crystals, Monte Carlo simulated annealing[19] was applied with the COMPASSII force field[20] and the following parameters: a maximum number of 10000 steps, 14 steps to accept before cooling, a minimum move factor of 10^{-10}, a cooling factor of 0.0005, and temperatures between 300 and 150 K. Point charges were

obtained from *ab initio* ESP calculations on a molecule optimized at the MP2/cc-pVDZ level of theory, and long-range interactions were treated with the Ewald summation method with an accuracy of 0.001 kcal/mol. We investigated five of the most common space groups (*P1*, *C2/c*, *P2_1*, *P2_12_12_1*, and *P2_1/c*) for organic molecules and space group *Pc* according to experimental observations.[21] The lattice and atomic positions were then optimized with the molecular mechanics Smart algorithm using an energy criterion of 0.002 kcal/mol; the redundant polymorphs were eliminated, and the obtained structures were ranked on the basis of their potential energy. This part was done using the Polymorph Predictor module included in the Materials Studio software package.[22]

Periodic density functional theory (PW-DFT) investigations were then performed by using the PBE functional[23] and the Tkatchenko−Scheffler correction scheme[24] for treating van der Waals interactions (PBE-TS) with a γ-centered $4 \times 4 \times 4$ k-point grid to sample the reciprocal space for all structural optimizations, using tight convergence criteria of 10^{-7} and 10^{-4} for ionic and electronic relaxations, respectively. This PBE and TS scheme combination is widely used to optimize lattice parameters and reproduce experimental data.[11] However, as recent CSP studies have shown that the polymorph ranking can be further improved if an energy calculation is performed using a PBE0 hybrid functional[25] with the many-body dispersion scheme,[26] subsequent calculations were performed with PBE0-MBD on the structures optimized with PBE-TS,[18] using a $2 \times 2 \times 2$ k-point grid to optimize the computational resources. The DFT calculations involved in the CSP were performed using the VASP software, version 5.4.4.[27]

■ RESULTS AND DISCUSSION

To identify the initial polymorph of the as-delivered phenoxazine powder, an X-ray diffraction powder pattern was collected (Figure 2). The pattern reveals a series of diffraction
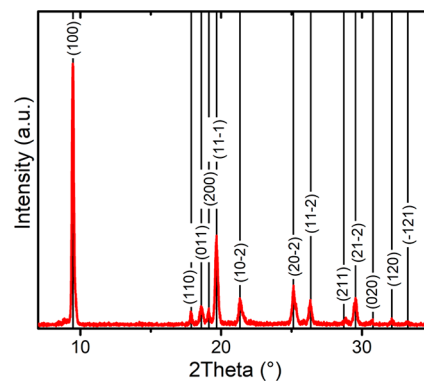

Figure 2. X-ray diffraction pattern of polycrystalline phenoxazine together with indexing of the observed Bragg peaks.

peaks, and the peak positions are used to index the pattern: i.e., to find a crystallographic unit cell that describes the position of the observed diffraction peaks. This was done by using the DICVol04 software suite.[28] The results give a monoclinic unit cell (see Table 1), which agrees well with values provided by the single-crystal solution below, except for the thermal expansion differences. Please note that the commercial powder was measured at room temperature.

Experimental Crystal Structure. To solve the crystal structure of phenoxazine, single-crystal X-ray diffraction was performed at a temperature of 100 K. The result reveals that phenoxazine crystallized in space group $P2_1/c$ with two planar molecules arranged in the unit cell (Table 1).

Further, one inversion center located at the center of the molecule is present, predicting that a substitutional disorder

Table 1. Summary of Crystallographic Data of the Phenoxazine Crystal Structure from Experimental X-ray Diffraction Studies (Polycrystalline Powder and Single Crystal) and Crystal Structure Predictions with PBE0MBD Using Two Different Space Groups

	polycrystalline powder	single crystal	crystal prediction $P2_1$	crystal prediction Pc
formula	$C_{12}H_9NO$	$C_{12}H_9NO$	$C_{12}H_9NO$	$C_{12}H_9NO$
temp (K)	293	100	0	0
crystal system	monoclinic	monoclinic	monoclinic	monoclinic
space group		$P2_1/c$	$P2_1$	Pc
a (Å)	9.51	9.335(2)	9.243(2)	9.281(6)
b (Å)	5.805	5.768(1)	5.673(4)	5.650(5)
c (Å)	8.522	8.261(2)	8.208(6)	8.229(8)
α (deg)	90	90	90	90
β (deg)	103.8	103.17(3)	102.61(3)	102.99(2)
γ (deg)	90	90	90	90
V (Å^3)	456.9	433.11	420.074	420.57
Z		2	2	2
ρ (g cm^{-3})	1.332	1.405	1.449	1.447
packing motif		herringbone	herringbone	herringbone
crystal habit	plate	plate		
no. of rflns measd	13	7826		
R1($I > 2\sigma(I)$)		0.0523		
wR2($I > 2\sigma(I)$)		0.1518		

exists between oxygen and nitrogen atoms over two positions. The consideration of the molecular structure and the observed packing, together with the space group found, result in an occupancy factor of 50% for each atom (oxygen and nitrogen) over the two sites. This partial occupation improved the overall agreement during the refinement process. The positions of hydrogen atoms were calculated from a known geometry and treated as riding with $U_{iso}(H) = 1.2U_{eq}(C)$.

Due to the observed symmetry, only one molecule has to be considered to analyze the packing scheme. The molecule is connected with four closest neighbors through C−H···N, C−H···O, and C−H···π short contacts to form a 2D network layer (marked in green in Figure 3a). However, the complete molecular environment has to be taken into account for a more detailed investigation of the intermolecular interactions. An improved visualization of the molecular interactions together with a quantitative evaluation of the different contributions to the molecular packing can be performed by a Hirshfeld surface analysis.[29,30] The X−H bond lengths in crystal structures solved by X-ray diffraction are underestimated, however, on the basis of the electronic density. To build Hirshfeld surfaces, CrystalExplorer thus normalizes the X−H bond lengths to those obtained from neutron diffraction experiments: i.e., 1.083 and 1.009 Å for C−H and N−H bonds, respectively. Those values are close to those obtained by the PBE-TS geometry optimizations (see Table S1). The Hirshfeld analysis is shown in Figure 3b−d by the molecular Hirshfeld surface, the 2D fingerprint, and quantitative contributions of different types of interaction between the molecules. As shown in Figure 3b, the large, vivid red spots at the Hirshfeld surface belong to localized C−H···N short contacts, which are represented with two spikes in the 2D fingerprint plots (Figure 3c) and have a contribution of 4.9% to the Hirshfeld surface (Figure 3d). Analyzing the numerous C···H interactions (representing C−H···π short contacts) reveals that only a few of them give rise to the smaller and less conspicuous red spots mingled with the main C−H···N red spot (Figure 3b), which on average reflects longer distances in comparison to those of C−H···N contacts. However, C···H contacts globally build up into a very large
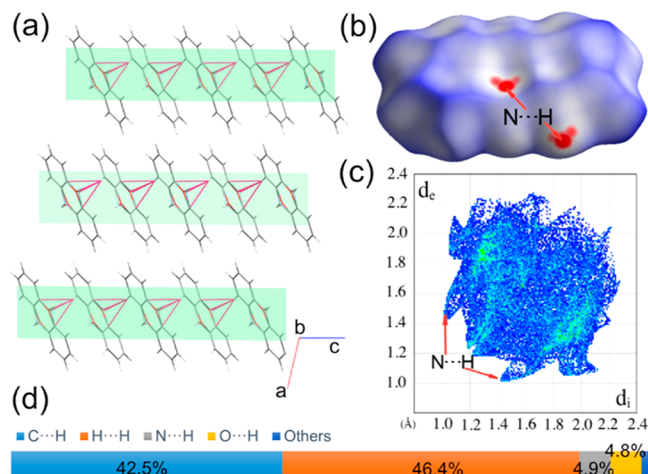

Figure 3. (a) Molecular packing of phenoxazine within the crystal structure. The dotted red lines indicate C−H···N and C−H···π intermolecular interactions. (b) Hirshfeld surface with d_{norm} over the range −0.1 to +1.3 plotted by a blue/white/red color code map representing distances larger/equal/smaller in comparison to the van der Waals distances, respectively. The characteristic C−H···N close contact is marked. (c) 2D fingerprint plot for phenoxazine. (d) Quantitative contribution of different short contacts to the surface as obtained at the PBE-TS level.

contribution of 42.5% (Figure 3d) to the interactions within the crystal structure. This analysis also points to the absence of any strong and significant H···O hydrogen-bonding interaction.

In summary, the phenoxazine molecules show a planar conformation within the crystalline state and pack in a layered structure with a herringbone arrangement. This packing motif is frequently observed for rodlike conjugated molecules.[31]

Modeling of Substitutional Disorder. In a next step, the occupancy of oxygen and nitrogen has been theoretically investigated. The simulations start from the experimental results with a 50%:50% occupancy ratio for the oxygen and nitrogen atoms at the sites (Figure 4a). With the assumption that the uncertainty in the site occupation disappears, the space
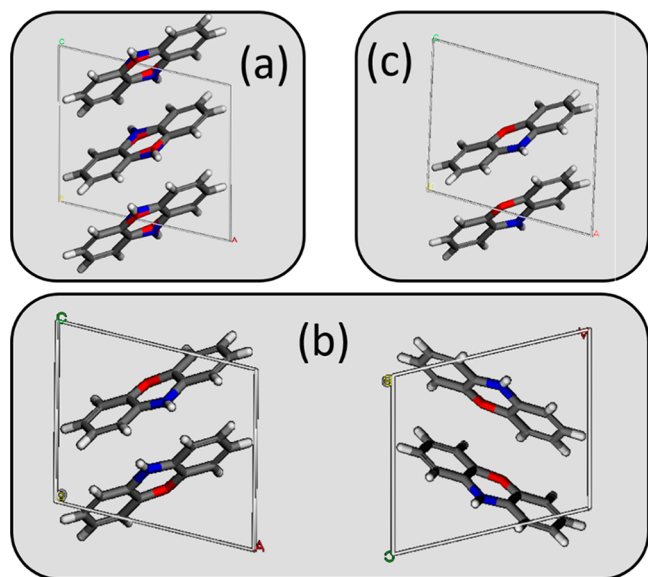
Figure 4. Different representations of the molecular packing within the bulk crystal structure of phenoxazine: (a) experimental structure with random site occupancy of oxygen (red) and nitrogen (blue); (b) the two types of regular site occupancy within the space group $P2_1$; (c) the regular site occupancy within the space group Pc.

group $P2_1/c$ is modified to $P2_1$ and Pc due to the reduction of the symmetry operations. Defined positions of oxygen and nitrogen atoms lead to three different structures: two structures that are enantiomers in space group $P2_1$ and another structure in space group Pc. Only one structure can be obtained in the Pc space group due to the glide plane symmetry operation. The three structures were fully optimized using DFT at the PBE-TS level. The two structures belonging to the same space group $P2_1$ have the same energy, as expected, whereas the Pc structure is 0.4 kJ/mol more stable than the $P2_1$ structures. Note that in the entire text the energy is given per mole of molecules, not per mole of crystal cells. The two structures in $P2_1$ and the structure in Pc are presented in Figure 4b,c, respectively. They differ only in the position of the oxygen/nitrogen atoms inside the unit cell, and no change of the molecular packing is observed by setting the positions of the oxygen and nitrogen atoms within the crystallographic unit cell. The theoretically predicted structures involve equivalent interactions, which explains why all of the structures (both $P2_1$ and Pc) have very similar energies. This result, in combination with the Hirshfeld surface analysis, confirms that the crystal packing of phenoxazine is mainly driven by weak van der Waals interactions, with a small percentage of short interactions between oxygen/nitrogen atoms and hydrogen atoms bound to carbon atoms.

To get further insight into the issue of substitutional disorder, a modeling study was carried out using a crystal structure prediction (CSP) approach, which is expected to provide a crystal structure landscape containing the thermodynamic phase observed.[18] The CSP started with the force-field method to generate more than 3000 candidate structures, after the redundant structures were eliminated. The structures with the lowest energy in a window of 10 kJ/mol were selected for DFT ranking. In total, 85 candidates were optimized at the PBE-TS level. Among them, we identified the two different groups of structures already discussed ($P2_1$ and Pc) and a third structure in $P2_1/c$, which has the same motif and lattice

parameters but with the a axis being twice as large. This structure is composed of two $P2_1$ enantiomers next to each other (below it is referred to as the "combined $P2_1/c$ structure"). We thus also considered a fourth structure, built similarly to this one, but using the Pc motif instead of the $P2_1$ motif.

Finally, the single-point energy calculations at the PBE0-MBD level were performed on the PBE-TS-optimized structures of a final pool of 16 candidates within an energy window of 4.2 kJ/mol. The two $P2_1$ structures, the structure in Pc, and the combined $P2_1/c$ structures all appeared in the final energy ranking (see Table 2). The Pc structure appears in the

Table 2. Relative Energies of the Different Polymorphs Discussed in the Text, as Obtained by PBE-TS Optimization and PBE0-MBD Single-Point Energy Calculations

	PBE-TS (kJ/mol)	PBE0-MBD (kJ/mol)
Pc	0.18	0.00
$P2_1/c$, Pc	0.00	2.80
$P2_1$ enantiomers	0.56	0.61
$P2_1/c$, $P2_1$	0.18	3.24

first position; it is the most stable polymorph. The two isoenergetic structures in $P2_1$ come next, 0.6 kJ/mol higher than Pc, and the combined $P2_1/c$ structures come at higher energies, 2.8 and 3.2 kJ/mol for the Pc- and $P2_1$-related motifs, respectively.

The data for the two significant structures (namely $P2_1$ and Pc) are given in Table 1. The theoretical and experimental results of the molecular packing match quite remarkably. The Pc structure is more likely to occur than the others, but that structure cannot explain an occupancy factor of 50% for oxygen and nitrogen over the two sites. It is possible that the investigated single crystal has different domains of phenoxazine molecules in its solid forms. The isoenergetic character of the $P2_1$ structures in the CSP ranking indicates that they have the same probability of being observed. Different $P2_1$ domains within the single crystal could thus explain averaged positions. However, an occupation factor of exactly 50% makes the presence of different $P2_1$ domains unlikely. This structure is also slightly higher in energy than the Pc structure. The combined $P2_1/c$ structures would explain an occupation factor of exactly 50%, but the crystal structure prediction reveals a doubled a axis for this case and a still higher energy value. In summary, these theoretical simulations suggest that an occupational O/N–H random disorder is more likely to explain an occupancy factor of 50% for these two groups.

■ CONCLUSION

The structure determination of phenoxazine is based on the single-crystal X-ray diffraction data. The unit cell parameters of the single crystal at a temperature of 100 K differs from those of X-ray powder diffraction results at room temperature due to a thermal expansion (Table 1); thus, it can be concluded that they represent the same polymorph. Phenoxazine crystallizes in monoclinic space group $P2_1/c$, and two molecules are present within the unit cell. Experimentally, a static disorder is found, which is manifested by the fact that two different orientations of phenoxazine molecules are present: i.e., half of them are oriented in one way while the other half take the opposite orientation. This results in an occupation factor of 50% for oxygen and the NH group. A crystal structure prediction was

performed to shed light on this observation, and the molecular packing analysis reveals cell parameters and structures in excellent agreement with those observed experimentally, except that the O and N−H positions are perfectly determined: a Pc structure is found to be slightly more stable than enantiomeric $P2_1$ structures. It is thus suggested that the occupancy factor of 50% is an occupational O/N−H disorder in the cell.

This study reveals that the phenoxazine molecule behaves in many respects like other rodlike conjugated molecules. The molecule shows an average planar conformation, and the crystal structure shows the well-known herringbone arrangement. Although the molecule has the possibility for intermolecular hydrogen bonding between the oxygen and NH group, this interaction does not influence the packing, so that the classical herringbone packing—typical for aromatic molecules—is observed.

■ ASSOCIATED CONTENT

ⓈI Supporting Information

The Supporting Information is available free of charge at https://pubs.acs.org/doi/10.1021/acs.cgd.1c00691.

> Intramolecular distances of C−H and N−H bonds obtained by different methods, energies of the intermolecular interaction for phenoxazine within the crystal structure, and the energy landscape for the different crystal structures (PDF)

> Crystallographic data for the experimentally determined structure with space group $P2_1/c$ (CIF)

> Crystallographic data for a theoretically optimized structure with space group Pc (CIF)

> Crystallographic data for a theoretically optimized structure with space group $P2_1$ (CIF)

Accession Codes

CCDC 2035887 contains the supplementary crystallographic data for this paper. These data can be obtained free of charge via www.ccdc.cam.ac.uk/data_request/cif, or by emailing data_request@ccdc.cam.ac.uk, or by contacting The Cambridge Crystallographic Data Centre, 12 Union Road, Cambridge CB2 1EZ, UK; fax: +44 1223 336033.

■ AUTHOR INFORMATION

Corresponding Author

Roland Resel − Institute of Solid State Physics, University of Technology Graz, 8010 Graz, Austria; ⓞ orcid.org/0000-0003-0079-3525; Email: roland.resel@tugraz.at

Authors

Martin Kaltenegger − Laboratoire de Chimie des Polymères, Faculté des Sciences, Université Libre de Bruxelles (ULB), 1050 Bruxelles, Belgium; Institute of Solid State Physics, University of Technology Graz, 8010 Graz, Austria

Louis Delaive − Laboratory for Chemistry of Novel Materials, Materials Research Institute, University of Mons, 7000 Mons, Belgium

Sai Manoj Gali − Laboratory for Chemistry of Novel Materials, Materials Research Institute, University of Mons, 7000 Mons, Belgium; ⓞ orcid.org/0000-0002-0388-7888

Patrick Brocorens − Laboratory for Chemistry of Novel Materials, Materials Research Institute, University of Mons, 7000 Mons, Belgium

Oliver Werzer − Department for Pharmaceutical Technology and Biopharmacy, Institute Pharmaceutical Sciences, Graz University, 8010 Graz, Austria

Hans Riegler − Department for Pharmaceutical Technology and Biopharmacy, Institute Pharmaceutical Sciences, Graz University, 8010 Graz, Austria

Yves Henri Geerts − Laboratoire de Chimie des Polymères, Faculté des Sciences, Université Libre de Bruxelles (ULB), 1050 Bruxelles, Belgium; International Solvay Institutes of Physics and Chemistry, 1050 Brussels, Belgium; ⓞ orcid.org/0000-0002-2660-5767

Roberto Lazzaroni − Laboratory for Chemistry of Novel Materials, Materials Research Institute, University of Mons, 7000 Mons, Belgium; ⓞ orcid.org/0000-0002-6334-4068

Jie Liu − Laboratoire de Chimie des Polymères, Faculté des Sciences, Université Libre de Bruxelles (ULB), 1050 Bruxelles, Belgium; ⓞ orcid.org/0000-0002-1301-057X

Complete contact information is available at:
https://pubs.acs.org/10.1021/acs.cgd.1c00691

Author Contributions

H.R. prepared the single crystal. M.K. performed X-ray powder diffraction and indexed the diffraction pattern. O.W. and J.L. solved the crystal structure from experimental data. L.D., S.M.G., P.B. and R.L. were responsible for the theoretical calculations. J.L. calculated and analyzed the Hirshfeld surface. M.K., Y.G., and R.R. prepared the first version of the manuscript. All authors have given their approval to the final version of the manuscript.

Notes

The authors declare no competing financial interest.

■ ACKNOWLEDGMENTS

■ REFERENCES

(1) Katsamakas, S.; L. Zografos, A.; Sarli, V. Advances of Phenoxazines: Synthesis, Reactivity and Their Medicinal Applications. Curr. Med. Chem. 2016, 23 (26), 2972−2999.

(2) Onoabedje, E. A.; Egu, S. A.; Ezeokonkwo, M. A.; Okoro, U. C. Highlights of Molecular Structures and Applications of Phenothiazine & Phenoxazine Polycycles. J. Mol. Struct. 2019, 1175, 956−962.

(3) Singhabhandhu, A.; Robinson, P. D.; Fang, J. H.; Geiger, W. E. Crystal and Molecular Structures of Ion Radical Molecular Complexes of Cis-Bis(Trifluoromethylethylene-1,2-Dithiolato)Nickel with Phenothiazine and Phenoxazine. Effects of Donor-Acceptor Separation on the Molecular Properties. Inorg. Chem. 1975, 14 (2), 318−323.

(4) Vogt, F. G.; Vena, J. A.; Chavda, M.; Clawson, J. S.; Strohmeier, M.; Barnett, M. E. Structural Analysis of 5-Fluorouracil and Thymine Solid Solutions. J. Mol. Struct. 2009, 932 (1−3), 16−30.

(5) Florence, A. J.; Leech, C. K.; Shankland, N.; Shankland, K.; Johnston, A. Control and Prediction of Packing Motifs: A Rare

Occurrence of Carbamazepine in a Catemeric Configuration. *CrystEngComm* **2006**, *8* (10), 746.

(6) Britton, D. Planar Packing of Tetrachlorodicyanobenzenes. II. *Acta Crystallogr. B* **2009**, *65* (1), 54−58.

(7) Müller, P. Practical Suggestions for Better Crystal Structures. *Crystallogr. Rev.* **2009**, *15* (1), 57−83.

(8) Habgood, M.; Grau-Crespo, R.; Price, S. L. Substitutional and Orientational Disorder in Organic Crystals: A Symmetry-Adapted Ensemble Model. *Phys. Chem. Chem. Phys.* **2011**, *13* (20), 9590.

(9) Lusi, M. Engineering Crystal Properties through Solid Solutions. *Cryst. Growth Des.* **2018**, *18* (6), 3704−3712.

(10) Dittrich, B.; Sever, C.; Lübben, J. Disappearing Disorder. *CrystEngComm* **2020**, *22* (43), 7432−7446.

(11) Binns, J.; Healy, M. R.; Parsons, S.; Morrison, C. A. Assessing the Performance of Density Functional Theory in Optimizing Molecular Crystal Structure Parameters. *Acta Crystallogr. Sect. B Struct. Sci. Cryst. Eng. Mater.* **2014**, *70* (2), 259−267.

(12) Kabsch, W. XDS. *Acta Crystallogr. D Biol. Crystallogr.* **2010**, *66* (2), 125−132.

(13) Winn, M. D.; Ballard, C. C.; Cowtan, K. D.; Dodson, E. J.; Emsley, P.; Evans, P. R.; Keegan, R. M.; Krissinel, E. B.; Leslie, A. G. W.; McCoy, A.; McNicholas, S. J.; Murshudov, G. N.; Pannu, N. S.; Potterton, E. A.; Powell, H. R.; Read, R. J.; Vagin, A.; Wilson, K. S. Overview of the *CCP* 4 Suite and Current Developments. *Acta Crystallogr. D Biol. Crystallogr.* **2011**, *67* (4), 235−242.

(14) Evans, P. R.; Murshudov, G. N. How Good Are My Data and What Is the Resolution? *Acta Crystallogr. D Biol. Crystallogr.* **2013**, *69* (7), 1204−1214.

(15) Sheldrick, G. M. A Short History of *SHELX*. *Acta Crystallogr. A* **2008**, *64* (1), 112−122.

(16) Wolff, S. K.; Grimwood, D. J.; McKinnon, J. J.; Turner, M. J.; Jayatilaka, D.; Spackman, M. A. *CrystalExplorer 17.5*; University of Western Australia: 2012.

(17) Neumann, M. A.; Perrin, M.-A. Energy Ranking of Molecular Crystals Using Density Functional Theory Calculations and an Empirical van Der Waals Correction. *J. Phys. Chem. B* **2005**, *109* (32), 15531−15541.

(18) Hoja, J.; Ko, H.-Y.; Neumann, M. A.; Car, R.; DiStasio, R. A.; Tkatchenko, A. Reliable and Practical Computational Description of Molecular Crystal Polymorphs. *Sci. Adv.* **2019**, *5* (1), eaau3338.

(19) Akkermans, R. L. C.; Spenley, N. A.; Robertson, S. H. Monte Carlo Methods in Materials Studio. *Mol. Simul.* **2013**, *39* (14−15), 1153−1164.

(20) Sun, H.; Jin, Z.; Yang, C.; Akkermans, R. L. C.; Robertson, S. H.; Spenley, N. A.; Miller, S.; Todd, S. M. COMPASS II: Extended Coverage for Polymer and Drug-like Molecule Databases. *J. Mol. Model.* **2016**, *22* (2), 47.

(21) Bond, A. D. Automated Derivation of Structural Class Symbols and Extended Z′ Descriptors for Molecular Crystal Structures in the Cambridge Structural Database. *CrystEngComm* **2008**, *10*, 411−415.

(22) *BIOVIA Materials Studio*; Dassault Systèmes: 2019.

(23) Perdew, J. P.; Burke, K.; Ernzerhof, M. Generalized Gradient Approximation Made Simple. *Phys. Rev. Lett.* **1996**, *77* (18), 3865−3868.

(24) Tkatchenko, A.; Scheffler, M. Accurate Molecular Van Der Waals Interactions from Ground-State Electron Density and Free-Atom Reference Data. *Phys. Rev. Lett.* **2009**, *102* (7), 073005.

(25) Perdew, J. P.; Ernzerhof, M.; Burke, K. Rationale for Mixing Exact Exchange with Density Functional Approximations. *J. Chem. Phys.* **1996**, *105* (22), 9982−9985.

(26) Tkatchenko, A.; DiStasio, R. A.; Car, R.; Scheffler, M. Accurate and Efficient Method for Many-Body van Der Waals Interactions. *Phys. Rev. Lett.* **2012**, *108* (23), 236402.

(27) Kresse, G.; Furthmüller, J. Efficient Iterative Schemes for *Ab Initio* Total-Energy Calculations Using a Plane-Wave Basis Set. *Phys. Rev. B* **1996**, *54* (16), 11169−11186.

(28) Boultif, A.; Louër, D. Powder Pattern Indexing with the Dichotomy Method. *J. Appl. Crystallogr.* **2004**, *37* (5), 724−731.

(29) Spackman, M. A.; McKinnon, J. J. Fingerprinting Intermolecular Interactions in Molecular Crystals. *CrystEngComm* **2002**, *4* (66), 378−392.

(30) McKinnon, J. J.; Jayatilaka, D.; Spackman, M. A. Towards Quantitative Analysis of Intermolecular Interactions with Hirshfeld Surfaces. *Chem. Commun.* **2007**, *37*, 3814.

(31) Desiraju, G. R.; Gavezzotti, A. Crystal Structures of Polynuclear Aromatic Hydrocarbons. Classification, Rationalization and Prediction from Molecular Structure. *Acta Crystallogr. B* **1989**, *45* (5), 473−482.